*Journal of Veterinary Science*

JVS

## Original Article
### Regenerative Medicine

Check for updates

# Immunosuppression-enhancing effect of the administration of allogeneic canine adipose-derived mesenchymal stem cells (cA-MSCs) compared with autologous cA-MSCs *in vitro*

**Hayeon Wi** [iD], **Seunghoon Lee** [iD], **Youngim Kim** [iD], **Jin-Gu No** [iD], **Poongyeon Lee** [iD], **Bo Ram Lee** [iD], **Keon Bong Oh** [iD], **Tai-young Hur** [iD], **Sun A Ock** [iD] *

Animal Biotechnology Division, National Institute of Animal Science, Rural Development Administration, Wanju 55365, Korea

OPEN ACCESS

**\*Corresponding author:**
**Sun A Ock**
Animal Biotechnology Division, National Institute of Animal Science, Rural Development Administration, 1500 Kongjwipatjwi-ro, Iseo-myeon, Wanju 55365, Korea.
E-mail: ocksamoon@gmail.com
          ocksa@korea.kr

**ORCID iDs**
Hayeon Wi [iD]
https://orcid.org/0000-0001-5008-4626
Seunghoon Lee [iD]
https://orcid.org/0000-0002-4362-7538
Youngim Kim [iD]
https://orcid.org/0000-0002-3926-5909
Jin-Gu No [iD]
https://orcid.org/0000-0002-7851-7662
Poongyeon Lee [iD]
https://orcid.org/0000-0003-2447-0392

## ABSTRACT

**Background:** Recently, mesenchymal stem cells therapy has been performed in dogs, although the outcome is not always favorable.

**Objectives:** To investigate the therapeutic efficacy of mesenchymal stem cells (MSCs) using dog leukocyte antigen (DLA) matching between the donor and recipient *in vitro*.

**Methods:** Canine adipose-derived MSCs (cA-MSCs) isolated from the subcutaneous tissue of Dog 1 underwent characterization. For major DLA genotyping (DQA1, DQB1, and DRB1), peripheral blood mononuclear cells (PBMCs) from two dogs (Dogs 1 and 2) were analyzed by direct sequencing of polymerase chain reaction (PCR) products. The cA-MSCs were co-cultured at a 1:10 ratio with activated PBMCs (DLA matching or mismatching) for 3 days and analyzed for immunosuppressive (*IDO*, *PTGS2*, and *PTGES*), inflammatory (*IL6* and *IL10*), and apoptotic genes (*CASP8*, *BAX*, *TP53*, and *BCL2*) by quantitative real-time reverse transcriptase-PCR.

**Results:** cA-MSCs were expressed cell surface markers such as CD90$^+$/44$^+$/29$^+$/45$^-$ and differentiated into osteocytes, chondrocytes, and adipocytes *in vitro.* According to the Immuno Polymorphism Database, DLA genotyping comparisons of Dogs 1 and 2 revealed complete differences in genes DQA1, DQB1, and DRB1. In the co-culturing of cA-MSCs and PBMCs, DLA mismatch between the two cell types induced a significant increase in the expression of immunosuppressive (*IDO/PTGS2*) and apoptotic *(CASP8/BAX)* genes.

**Conclusions:** The administration of cA-MSCs matching the recipient DLA type can alleviate the need to regulate excessive immunosuppressive responses associated with genes, such as *IDO* and *PTGES.* Furthermore, easy and reliable DLA genotyping technology is required because of the high degree of genetic polymorphisms of DQA1, DQB1, and DRB1 and the low readability of DLA 88.

**Keywords:** Dog; allogeneic transplantation; adipose-derived mesenchymal stem cells; leukocyte antigen; immunosuppressive

Generated by xmlinkpress

Bo Ram Lee [iD]
https://orcid.org/0000-0002-0537-6205
Keon Bong Oh [iD]
https://orcid.org/0000-0002-0651-0306
Tai-young Hur [iD]
https://orcid.org/0000-0003-3129-2942
Sun A Ock [iD]
https://orcid.org/0000-0002-0887-8200

**Conflict of Interest**

The authors declare no conflicts of interest.

**Author Contributions**

Conceptualization: Wi H, Ock SA; Data curation: Wi H, Ock SA; Formal analysis: Wi H; Funding acquisition: Wi H; Investigation: Wi H, Kim Y, Ock SA; Methodology: Lee S, No JG, Lee BR, Oh KB, Hur TY; Project administration: Lee P, Hur TY; Supervision: Lee P, Hur TY, Ock SA; Validation: Ock SA; Writing - original draft: Wi H; Writing - review & editing: Ock SA.

# INTRODUCTION

In regenerative medicine, mesenchymal stem/stromal cells (MSCs) plasticity facilitated their therapeutic use for diseases that are difficult to treat using modern medicine in veterinary hospitals [1]. Additionally, MSC therapy is gaining interest due to the increasing prevalence of immune-related diseases, which exert immunomodulatory, immunosuppressive, and anti-inflammatory effects [2,3]. Canine adipose-derived MSCs (cA-MSCs) or bone marrow-derived MSCs for the treatment of atopic dermatitis and inflammatory bowel disease are being evaluated [1,2].

Among the major histocompatibility complex (MHC) classes, classes I and II are responsible for inducing major adaptive immune responses. In general grafting, human leukocyte antigen (HLA) is used in human MHC matching between a donor and recipient; it is a major factor that reduces serious postoperative complications, such as graft versus host disease (GvHD), graft failure, and immune rejection. However, HLA expression differs by cell type. Stem cells, for example, exhibit low HLA class I expression and lack HLA class II [4]. Similarly, in MSCs, HLA class I expression and HLA class II silencing did not affect the response of CD4$^+$ T cells as key adaptive immune response factors [5,6].

Allogeneic MSCs can be therapeutically effective; they can be collected through *in vivo* cultures of young and healthy cell sources and cryopreserved, reducing the waiting time for treatment in seriously ill patients [1]. However, allogeneic MSCs pose certain risks, including graft rejection and GvHD. Autologously derived cells for MSC therapy do not induce an immune response. There is no risk of GvHD or the need to identify a donor; however, the source of cells may be limited due to disease or aging, and therapy requires cell culturing and expansion *in vitro*. Although MSCs have immunomodulatory capacity, they can be reactivated under *in vitro* culture conditions, which can induce negative results during *in vivo* therapy [4,7,8].

Canines produce dog leukocyte antigens (DLAs); like HLA, the gene coding for DLA is located on chromosome 12. DLA plays a role in immune recognition of donor and recipient materials, and DLA class II MHCs are highly polymorphic [9,10]. However, early studies of MSC therapy did not consider DLA matching between donors and recipients, and conflicting results have been reported [11-14].

Based on DLA genotyping analyses, this study aimed to evaluate whether canine MSCs transfused as autografts or allografts *in vitro* induced immune responses, such as immunosuppression and inflammation-induced cytokine secretion. Adipose tissues were selected as the source of MSCs for this study, as the guardians of the animals were less likely to object to adipose tissue collection. cA-MSCs were co-cultured with peripheral blood mononuclear cells (PBMCs) with a matched or mismatched DLA genotype. Immunosuppressive and inflammatory gene expression was analyzed in MSCs and treated PBMCs. Additionally, this study confirmed the validity of the previously reported DLA genotyping methods.

# MATERIALS AND METHODS

## Experimental materials

Subcutaneous adipose tissues and peripheral blood (Orient Bio Co. Ltd., Korea) of two healthy 4-month-old male dogs (Covance Beagles; Covance Inc., USA) were used in this

study, which was approved by the Institutional Animal Care and Use Committee of the National Institute of Animal Science (NIAS20181426).

### Chemicals and media
All chemicals and media were purchased from Sigma Aldrich (USA) and Thermo Fisher (USA). Any exceptions are indicated.

### Canine cell isolation
Cells were isolated from canine subcutaneous adipose tissue [15], using a combination of digestion with 0.25% collagen type I (Millipore, USA) and sequential filtration using 100 and 40 μm cell strainers (Corning Inc., USA). Isolated cells were seeded on 35 mm dishes and cultured in advanced Dulbecco's Modified Eagle Medium (ADMEM) containing 10% fetal bovine serum and 1% penicillin-streptomycin in a humidified 5% $CO_2$ incubator at 38.5℃ for 1 h. The culture medium was exchanged with fresh ADMEM to remove non-adherent cells every 3 days. Rapidly attached cells were cultured until 80% confluence at a sub-cultured 1:4 ratio. Cells were cultured until passage 5.

### Alkaline phosphatase (ALP) activity staining
At passage 2, cells grown in 4-well dishes (Nunc, Denmark) were used for ALP activity staining. Cells were fixed with 4% formaldehyde and stained using an ALP chromogen kit (ab7468; Abcam, UK) for 1 h at room temperature. ALP-positive reactions, assessed under an inverted microscope, were indicated by the appearance of purple-red.

### Flow cytometric cluster of differentiation (CD) marker analysis
Cells at passage two were detached with 0.25% trypsin-ethylenediaminetetraacetic acid and washed with phosphate-buffered saline (PBS) (pH 7.2). The concentration of suspended single cells was adjusted to $1 \times 10^6$ cells/mL, followed by incubation with anti-CD90-APC (Invitrogen, USA), anti-CD44-FITC (Santa Cruz Biotechnology, USA), anti-CD29-FITC (Thermo Fisher), and anti-CD45-Alexa Fluor488 (Bio-Rad, USA) antibodies at a 1:100 dilution in the dark for 1 h. The following isotype controls were used: immunoglobulin (Ig) G2b-APC (Invitrogen) for CD90, IgG2b-FITC (Santa Cruz Biotechnology) for CD44, IgG-FITC (Thermo Fisher) for CD29, and IgG2b-Alexa Fluor488 (AbD Serotec; Bio-Rad) for CD45. Flow cytometric (FACSCanto; Becton-Dickinson, USA) analysis was performed by reading 10,000 cells/sample. Data were acquired using FlowJo software (Tree Star, USA).

### Pluripotent marker analysis
Cells at passage two were fixed with 4% formaldehyde for 5 min, washed with PBS containing 0.1% Triton X-100, and incubated in 1:100 dilutions of specific antibodies with dog species reactivity, including anti-Oct 3/4 (sc9081; Santa Cruz Biotechnology, Japan), anti-SRY-box 2 transcription factor (SOX2) (SOX2 Monoclonal Antibody [20G5]; Thermo Fisher) or anti-Nanog homeobox (NANOG, ab77095; Abcam) at 4℃ overnight. Subsequently, cells were incubated in the following secondary antibody solutions for 1 h: Alexa Fluor 594-conjugated goat anti-rabbit IgG H&L (ab-150080; Abcam, 1:500) for Oct 3/4, Alexa Fluor 488-conjugated goat anti-mouse IgG (H+L) (A28175; Thermo Fisher, 1:200) for SOX2 or Alexa Fluor 488-conjugated donkey anti-goat IgG H&L (ab150129; Abcam, 1:200) for NANOG. Counterstaining was performed with 4′,6-diamino-2-phenylindole (DAPI) (Life Technologies, USA) for 1 h, followed by mounting with VECTASHIELD Antifade Mounting Media (Vector Laboratories, USA) and analysis under confocal laser scanning microscopy (Zeiss LSM880 Airyscan; Oberkochen, Germany).

### *In vitro* differentiation assay

To induce adipogenesis and osteogenesis, cells approaching up to 80% confluence on 35 mm dishes were differentiated using Adipogenesis (A1007001; Gibco StemPro, USA) or Osteogenesis Kits (A1007201; Gibco StemPro) according to the manufacturer's protocols for 4 weeks [16]. A 3-dimensional pellet culture system was adapted for chondrogenesis [17]. The pellets were formed with $1 \times 10^6$ cells in a 15 mL conical tube, and cells were differentiated with a Chondrogenesis Kit (A1007101; Gibco StemPro) for 4 weeks. Completely differentiated cell types were divided into groups for total RNA extraction and specific staining following fixation with 4% formaldehyde for 5 min.

Cells differentiated using an adipogenesis or osteogenesis kit were stained with 0.5% Oil Red O or Alizarin Red S for 1 h, respectively, and washed with PBS. The red color was observed as a positive reaction under a light microscope.

Pellets were sectioned with a cryotome (Cryomicrotome, Thermo Fisher) at a thickness of 8–10 μm and stained with Alcian blue solution (Lifeline Cell Technology, Oceanside, MD, USA) for 1 h to detect cartilage glycosaminoglycans. Sectioned samples were also subjected to double immunofluorescence labeling with anti-collagen type II (Abcam, 1:100) and anti-aggrecan monoclonal antibodies (Thermo Fisher, 1:100) at 4°C overnight, then incubated in the following secondary antibody solutions: goat anti-rabbit IgG H&L Alexa Fluor 594 (Abcam) and goat anti-mouse IgG (H+L) Alexa Fluor 488 (Thermo Fisher) for 1 h at 37°C. Counterstaining was performed with DAPI (Life Technologies) for 5 min at room temperature, followed by mounting with VECTASHIELD Antifade Mounting Media (Vector Laboratories) and observation under a light or confocal laser scanning microscopy (Zeiss LSM880 Airyscan; Oberkochen).

### DLA genotyping of PBMCs

PBMC isolation from the peripheral blood of dogs was performed according to the manufacturer's protocol using Ficoll-Paque PREMIUM 1.073 (GE Healthcare, USA). Recovered PBMCs were frozen at $1 \times 10^7$ cells/mL in 10% dimethyl sulfoxide (DMSO) and stored in liquid nitrogen. Total genomic DNA from PBMCs ($1 \times 10^7$ cells) was extracted using DNeasy Blood & Tissue Kits (Qiagen, Germany). Polymerase chain reaction (PCR) was performed using specific primers and methods for exon 2 of DLA-DQA1, DLA-DQB1, and DLA-DRB1, and for exons 1–3 of DLA-88 [18,19]. Genotyping of each PCR product was performed by direct sequencing. Alignment of allele sequences was performed using SeqMan software (DNASTAR Co, USA). The allele names were defined using the MHC Immuno Polymorphism Database (EMBL-EBI, UK).

### Mixed lymphocyte reaction test

PBMCs were pre-activated with phytohemagglutinin (PHA, 5 μg/mL) for three days. cA-MSCs were seeded at $0.2 \times 10^5$ cells/well in 24-well plates (Nunc) and cultured for 6 h. Subsequently, $2 \times 10^5$ PBMCs with or without pre-activation were seeded onto the cA-MSCs in each well and co-cultured for 3 days. At 1-day intervals, cA-MSCs and PBMCs were harvested for quantitative real-time reverse transcriptase-polymerase chain reaction (qRT-PCR) analysis. Samples harvested from the same experimental group were pooled for total RNA extraction.

### qRT-PCR

According to the manufacturer's protocol, total RNA was extracted using RNase Mini Kits (Qiagen). cDNA was synthesized from 500 ng of total RNA using Omniscript RT

**Table 1.** The list of primer sequences for real-time reverse transcriptase polymerase chain reaction experiments

| Gene | 5'-3' mRNA sequence | Accession number |
|---|---|---|
| Octamer-binding transcription factor 4/POU class 5 homeobox 1 (*OCT4*) | Forward: CAG ATC AGC CAC ATT GC<br>Reverse: CAC ACT CGG ACC ACA TCC TTC T | XM 538830.4 |
| SRY-box transcription factor 2 (*SOX2*) | Forward: CCC CTT TAT TTT CCG TAG TTG TAT TT<br>Reverse: GAT TCT CGG CAG ACT GAT TCA A | XM 005639752.4 |
| Nanog homeobox (*NANOG*) | Forward: TCA GGA CAG CCC GGA TTC T<br>Reverse: CCA GAG GTG GGT GGG AGT TT | XM 038437912.1 |
| Peroxisome proliferator activated receptor gamma (*PPARγ*) | Forward: GAA AAG CTG TTG GCG GAG AT<br>Reverse: CCG GAG ATC AGC CGA CTC T | NM 001024632.2 |
| Lipoprotein lipase (*LPL*) | Forward: GCC GTG GAG TGG GAA CAG<br>Reverse: GCC CGA AGT GGC TGG TT | XM 005635734.4 |
| Leptin (*LEP*) | Forward: ACC GTA TGG GTG TCC TTT ATC CT<br>Reverse: GAA GAG TGG CTC TGT GGT GTG A | NM 001003070.1 |
| Alkaline phosphatase (*ALP*) | Forward: GGC GTC CAC GAG CAG AAC<br>Reverse: CGA TGC AGG CCG CAT AA | NM 001197137.1 |
| Secreted phosphoprotein 1 (*SPP1*) | Forward: ACG AGT CTG ATG AAT CCG ATG AA<br>Reverse: AAT TGG GTT GCT GGA ATG TCA | XM 003434024.5 |
| Runt-related transcription factor 2 (*RUNX2*) | Forward: AAG CCC TCC TGT AGG ATG CA<br>Reverse: ACG CTT GAG AAT TTG CCA TGT | XM 038683679.1 |
| SRY-box transcription factor 9 (*SOX9*) | Forward: GCG TGC AGC ACA AGA AAG AC<br>Reverse: GGC CGT TCT TCA CCG ACT T | NM 001002978.1 |
| Aggrecan (*ACAN*) | Forward: CCG AGG CAA CGT GAT CCT<br>Reverse: CAT CGG TGG CGA AAG TGA A | NM 001113455.2 |
| Collagen type II alpha 1 chain (*COL2A1*) | Forward: CAT CGG GCC TGT CTG CTT<br>Reverse: ATT GGC AAT GGA TTG TGT TT | NM 001006951.1 |
| Indoleamine 2,3-dioxygenase (*IDO1*) | Forward: TGT GGA CCC AAG CAC GTT TT<br>Reverse: AGT TGC CTT TCC AAC CAG ACA | XM 038689794.1 |
| Prostaglandin-endoperoxide synthase 2 (*PTGS2*) | Forward: CGG CGA AAA CTG CTC AAC A<br>Reverse: TTG GAG TGG GTT TCA GGT ATA ATT T | NM 001003354.1 |
| Interleukin 6 (*IL-6*) | Forward: GAC CAC TCC TGA CCC AAC CA<br>Reverse: ATC CTG CGA CTG CAA GAT AGC | NM_001003301.1 |
| Interleukin 10 (*IL-10*) | Forward: CCC AGG ATG CAA CTC TTC TC<br>Reverse: CGG GAT GGT ATT TTG CAG ATC | NM_001003077.1 |
| Prostaglandin E synthase (*PTGES*) | Forward: GTG TGC GTG CTC CTT GGA T<br>Reverse: CTG ACA TCT CTA CGT GGT CCA ATC | NM 001122854.1 |
| Caspase-8 (*CASP8*) | Forward: CAG AGA CTC CAG GAA AAG AGA ATG T<br>Reverse: TCG AAA AGC AGC CTC CTT CA | NM 001048029.1 |
| BCL2-associated X, apoptosis regulator (*BAX*) | Forward: GGT GCC CCA GGA TGC A<br>Reverse: CCG ATG CGC TTG AGA CAT T | NM 001003011.1 |
| Tumor protein 53 (*TP53*) | Forward: CCG CGC TAT GGC CAT CTA TA<br>Reverse: CAG CGC ACA ACC T | NM 001389218.1 |
| B-cell lymphoma 2 apoptosis regulator (*BCL2*) | Forward: AAT CAA GTG TTC CGC GTG ACT<br>Reverse: TTA TTG GAT GTG CTT TGC ATT CTT | NM 001002949.1 |
| Hypoxanthine phosphoribosyltransferase 1 (*HPRT1*) | Forward: CGG CTT GCT CGA GAT GTG AT<br>Reverse: GAG CAC ACA GAG GGC TAC GAT | NM 001003357.2 |

Kits (Qiagen). qRT-PCR reactions were performed using the StepOnePlus Real-Time PCR system (Applied Biosystems, USA) with SYBR Green PCR master mix (Applied Biosystems), using each of the gene-specific forward and reverse primers (**Table 1**). Data were analyzed using the $_{\Delta\Delta}C_T$ method [20]. The cycling protocol was as follows: 40 cycles at 95℃ for 15 s, 60℃ for 1 min, melting curve stage at 95℃ for 15 sec, 60℃ for 1 min, and 95℃ for 15 sec. Hypoxanthine-guanine phosphoribosyltransferase *(HPRT)* was used as the endogenous control gene.

## Statistical analysis
Independent *t*-tests were used to compare 2 groups and comparisons of more than 2 groups were conducted using a one-way analysis of variance (ANOVA). Significant main effects were

followed up by Fisher's Least Significant Difference *post hoc* analyses. The *p* values < 0.05 were statistically significant. Statistical Package for the Social Sciences (SPSS) 25.0 software (IBM Corp., USA) was used. Data are displayed as relative quantification (RQ), and error bars indicate ± minimum or maximum RQ. All experiments were performed in triplicate.

# RESULTS

## Stemness and MSC-specific CD marker evaluations

The attached cells were spindle-shaped, with fibroblast-like morphology (**Fig. 1A and B**), exhibiting positive ALP activity, especially in colonies (**Fig. 1D**). We analyzed whether cA-MSCs expressed pluripotent stem cell markers, such as OCT3/4, SOX2, and NANOG, via
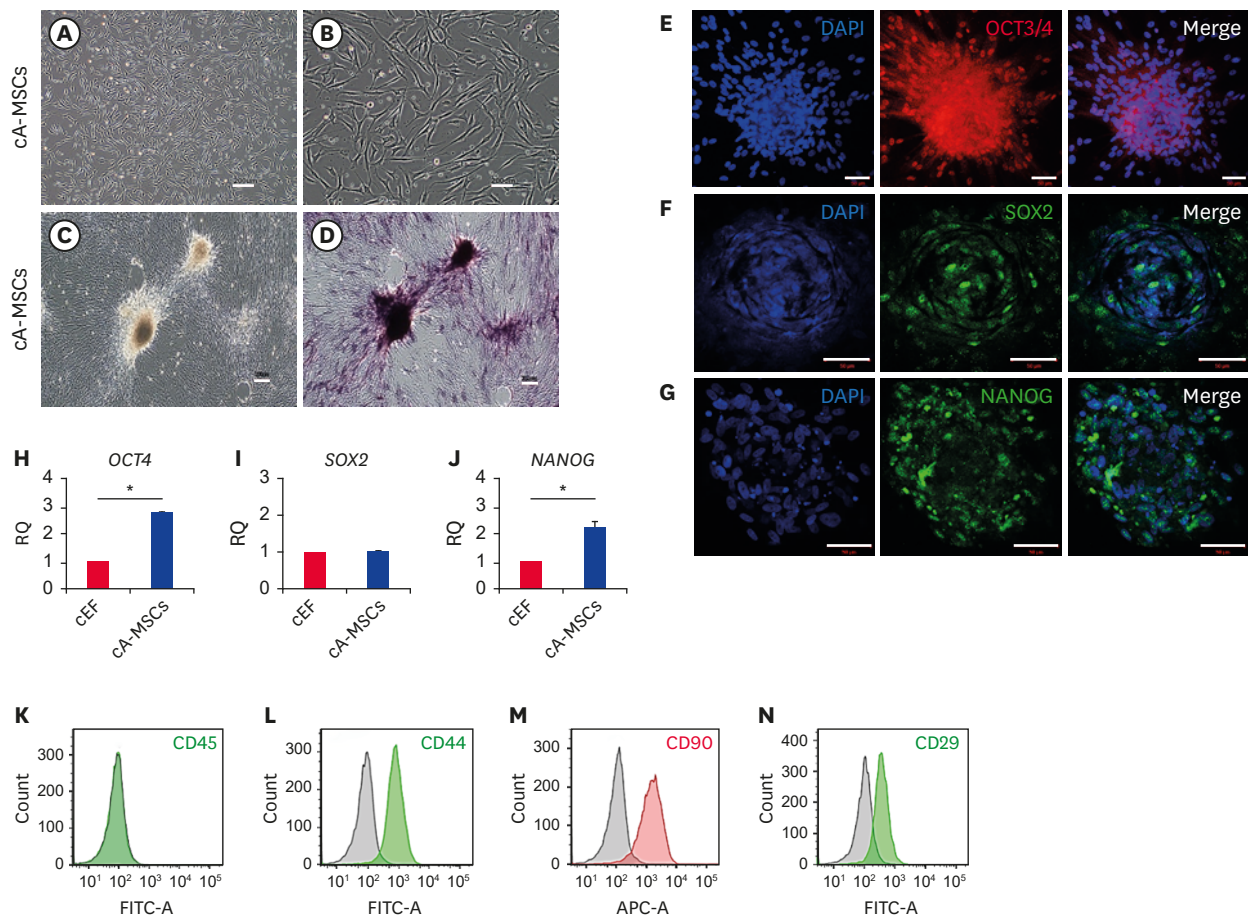


**Fig. 1.** Confirmation of MSC potency in cells derived from canine adipose tissue.
Morphological characteristics of canine adipose-derived cells from passage 0, observed at (A) low (scale bar = 200 μm) and (B) high (scale bar = 200 μm) magnification. Confirmation of ALP activity (C) before and (D) after ALP staining. Dark purple color denotes a positive chromogenic reaction indicating ALP activity (scale bars = 200 μm). (E-G) Expression of pluripotent proteins: (E) OCT3/4, (F) SOX2; and (G) NANOG, in canine adipose-derived cells. Green and blue colors indicate positive labeling and staining of cell nuclei by DAPI, respectively (scale bars = 50 μm). Quantification of mRNA expression of (H) *OCT4*, (I) *SOX2*, and (J) *NANOG* in canine adipose-derived cells (blue bars) by real time-polymerase chain reaction. cEF (red bars) were used as the negative control cells. All experiments were performed in triplicate. Error bars indicate the minimum and maximum values of RQ. Experiments (C-J) were performed with cells from passage 2. Expression of specific CD markers, (K) 45⁻, (L) 44⁺, (M) 90⁺, and (N) 29⁺ of MSCs in canine adipose-derived cells by flow cytometry. The red and green histograms indicate the expression levels of specific CD markers, and the black histogram represents those of the isotype-matched control. Cell concentrations were adjusted to $1 \times 10^6$ cells/mL, and readings were performed with 10,000 cells/sample. Changes in specific CD markers were calculated based on isotype-matched controls.
MSC, mesenchymal stem/stromal cell; ALP, alkaline phosphatase; *OCT3/4*, octamer-binding transcription factor 3/4; *SOX2*, SRY-box transcription factor 2; *NANOG*, Nanog homeobox; DAPI, 4′,6-diamino-2-phenylindole; cEF, canine ear fibroblasts; RQ, relative quantification of mRNA; CD, cluster of differentiation.
*$p$ < 0.05 indicates a significant difference between the two groups.

immunofluorescence labeling. All three proteins were expressed in the nuclei, although their expression was low (**Fig. 1E-G**). Colonies exhibited greater expression of the three proteins than did not colonial cells. The mRNA levels of both *OCT4* and *NANOG* were higher (2.7- and 2.2-fold, respectively) in cA-MSCs than in canine ear fibroblasts (cEF, control), although *SOX2* expression did not significantly differ between groups (**Fig. 1H-J**).

Analysis of expression patterns of MSC-specific CD markers revealed that they were negative for CD45, a hematopoietic marker (**Fig. 1K**), and positive for CD44 (94.1%), CD90 (87.2%), and CD29 (87.8%) (**Fig. 1L-N**). Thus, the cells were determined to be cA-MSCs.

### *In vitro* differentiation

In each differentiation induction medium, cA-MSCs were allowed to differentiate through adipogenesis, osteogenesis, or chondrogenesis for 4 weeks. Specific histochemical or immunochemical labeling and tissue-specific mRNA expression were subsequently analyzed.

In cA-MSC-induced adipogenesis, when cA-MSCs were stained with Oil Red O, red lipid droplets were observed in the cytoplasm (**Fig. 2A and B**). Quantification of the adipogenic markers peroxisome proliferator-activated receptor gamma (*PPARγ*), lipoprotein lipase (*LPL*), and leptin (*LEP*) revealed that differentiated cA-MSCs expressed significantly greater ($p < 0.05$) levels of *LEP* (260-fold), but not of *PPARγ* or *LPL* (**Fig. 2C**).

In cA-MSCs with induced osteogenesis, calcium accumulation was confirmed through positive Alizarin Red S staining (**Fig. 2D and E**). Quantification of the osteogenic markers secreted phosphoprotein 1 (*SPPI*), *ALP*, and Runt-related transcription factor 2 (*RUNX2*) revealed that, compared with controls, differentiated cA-MSCs expressed significantly ($p < 0.05$) greater levels of both *SPPI* (190-fold) and *RUNX2* (2-fold), but not *ALP* (**Fig. 2F**).

In cA-MSCs with induced chondrogenesis, morphological changes were confirmed based on changes in the shape of flattened cell pellets into spheroids (**Fig. 2H**). The spheroids, such as cartilage tissues, were fixed, cryosectioned, and stained with Alcian blue solution. The samples exhibited a positive Alcian blue reaction, especially on the spheroid surfaces (**Fig. 2I**). Positive immunolabeling of both aggrecan (green, as a cartilage-specific proteoglycan core protein, **Fig. 2M**) and collagen type II (red, a main component of cartilage, **Fig. 2L**) was confirmed using confocal microscopy. The expression of chondrogenic-related markers SRY-box transcription factor 9 (*SOX9*), Collagen type II alpha 1 chain (*COL2A1*), and Aggrecan (*ACAN*) were significantly increased in cA-MSCs compared with that of controls, especially *ACAN* (34.9-fold) (**Fig. 2J**).

### DLA analysis

DLA genotyping and matching analyses were performed using PBMCs from Dogs 1 and 2, which belonged to different family trees (**Fig. 3**). The reference genes used for genotyping of DLA-DQA1, DLA-DQB1, and DLA-DRB1 were DLA-DQA1*014012, DLA-DQB1*04201, and DLA-DRB*02002, respectively. Dog 1 was homozygous for DLA-DQA1 (*00101/*00101) and DLA-DQB1 (*0020/*00201), and heterozygous for DLA-DRB (*00101/*00201) (**Fig. 3D**). Dog 2 was heterozygous for DLA-DQA1 (*00402/*000401), DLA-DQB1 (*02301/*0301), and DLA-DRB1 (*04801/*01501) (**Fig. 3E**).

Between Dogs 1 and 2, inconsistent nucleotide sequences corresponding to single nucleotide polymorphisms (SNPs) were confirmed in the three DLA types, especially in DRB1, with the frequent appearance of SNPs at loci (**Fig. 3C**). However, genotyping of DLA 88 failed because
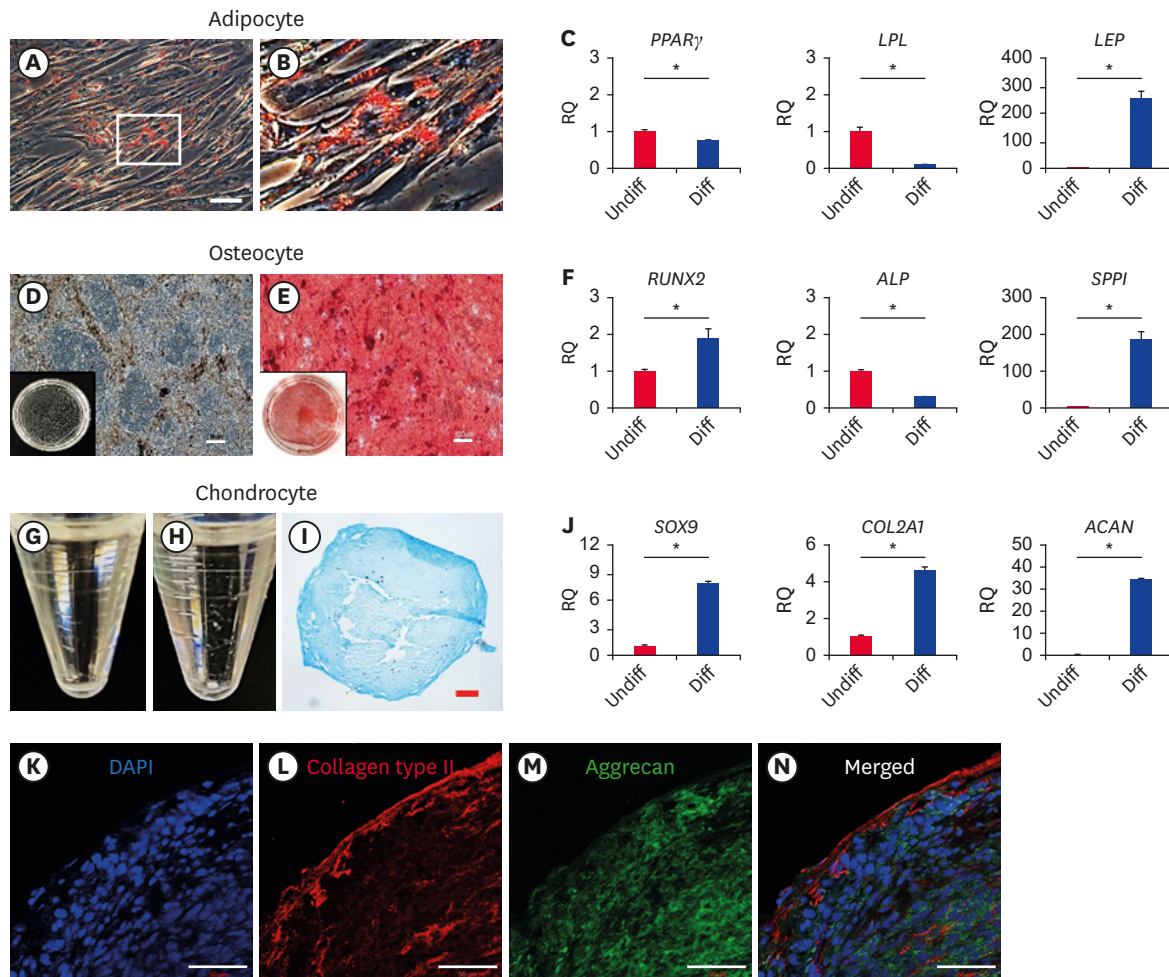
**Fig. 2.** *In vitro* differentiation of cells derived from canine adipose tissue.

Cells stained with Oil Red O after the induction of adipogenesis for 4 weeks. Red coloring denotes the presence of lipid droplets (A); the white box shows the borders of the enlarged inset shown in (B) (scale bars = 50 μm). (C) *PPARγ*, *LPL*, and *LEP* expression levels determined by real time-polymerase chain reaction in differentiated and undifferentiated cells. Cells stained with Alizarin Red S after inducing osteogenesis for 4 weeks. The red coloring is indicative of calcium and mineral accumulation. (D) and (E) represent samples before and after staining, respectively. Black boxes represent whole images of cells differentiated on a 35 mm dish (scale bars = 100 μm). (F) *RUNX2*, *ALP*, and *SPPI* expression levels determined by real time-polymerase chain reaction in differentiated and undifferentiated cells. Chondrogenesis induced in cells for 4 weeks. (G and H) represent cellular morphological changes before and after differentiation, respectively. (I) Section of a spheroid demonstrating positive Alcian blue staining used for detecting the presence of glycosaminoglycans (scale bars = 50 μm). (J), *SOX9*, *COL2A1*, and *ACAN* expression determined by real time-polymerase chain reaction in differentiated and undifferentiated cells. (K-N) A section of tissue positively labeled with anti-collagen type II (red, L) and anti-aggrecan (green, M) antibodies. Counterstaining of cell nuclei using DAPI is shown in (K), and the merge is shown in (N) (scale bars = 50 μm).

All experiments were performed in triplicate. Error bars indicate the minimum and maximum values of RQ.

*PPARγ*, proliferator-activated receptor gamma; *LPL*, lipoprotein lipase; *LEP*, leptin; *RUNX2*, Runt-related transcription factor 2; *ALP*, alkaline phosphatase; *SPPI*, secreted phosphoprotein 1; *SOX9*, SRY-box transcription factor 9; *COL2A1*, Collagen type II alpha 1 chain; *ACAN*, Aggrecan; DAPI, 4',6-diamino-2-phenylindole; RQ, relative quantification of mRNA.

*$p < 0.05$ indicates a significant difference between the 2 groups (before [red bars] and after [blue bars] differentiation).

no specific PCR product band was found at the expected DNA size following amplification. These results confirmed pedigree discrepancies between the two dogs.

## Immune reactions in cA-MSCs co-cultured with PBMCs

Immunomodulatory (indoleamine 2,3-dioxygenase [*IDO*] and prostaglandin-endoperoxide synthase 2 [*PTGS2*] and inflammation (*IL-10* and *IL-6*)-related genes were evaluated in cA-MSCs co-cultured with allogeneic (Dog 1) or autologous (Dog 2) PBMCs for 3 days (**Fig. 4B-G**). *IDO* expression was significantly ($p < 0.05$) increased in cA-MSCs co-cultured with allogeneic
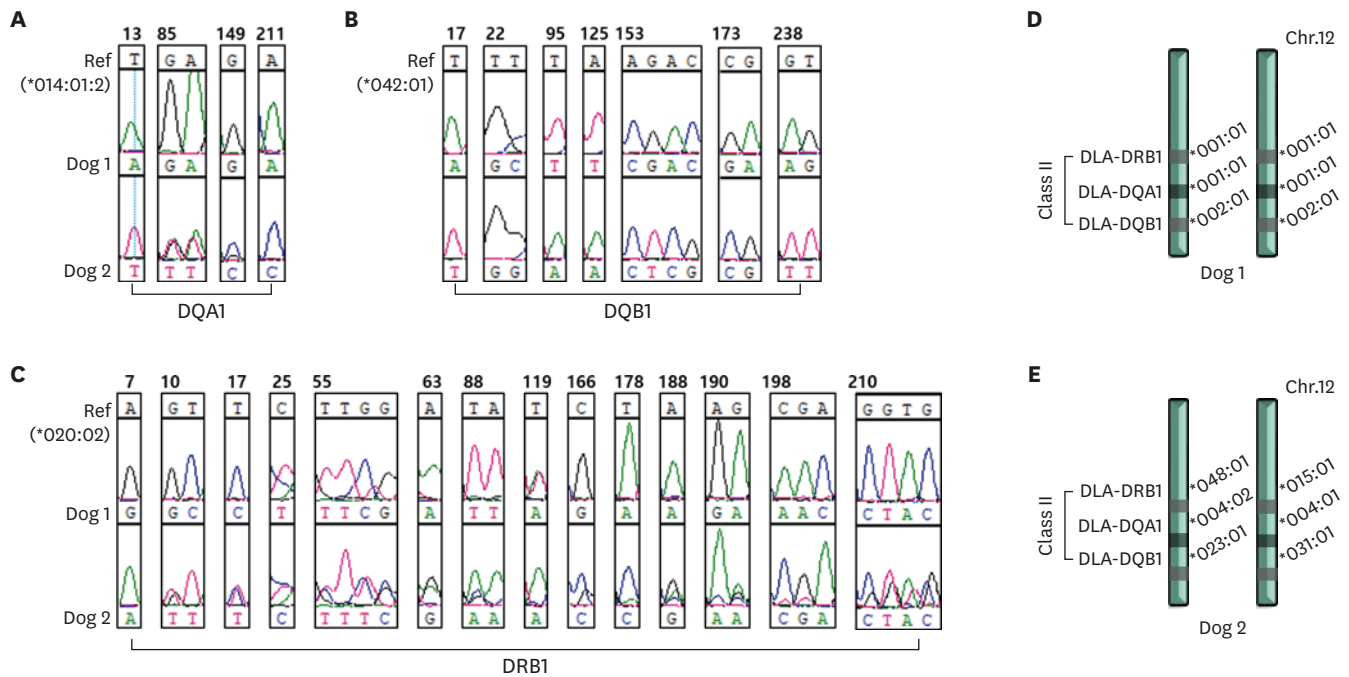
**Fig. 3.** Analysis of DLA types.
The DLA types of the 2 dogs analyzed concerning nucleotide alignment sequences based on reference genes: (A) *014012 for DQA1, (B) *04201 for DQB1, (C) *02002 for DRB1; the mismatched loci are displayed. Maps of the DLA genomic region on chromosome 12 and genotyping of DLA, displaying each allele of the 2 dogs, (D) Dog 1 and (E) Dog 2.
DLA, dog leukocyte antigen.

PBMCs (19.5-fold) regardless of PHA treatment; this did not occur in cA-MSCs co-cultured with autologous PBMCs. *PTGS2* was significantly ($p < 0.05$) upregulated (1.9-fold) in cA-MSCs co-cultured with activated allogeneic PBMCs compared with levels in cA-MSCs cultured alone. The expression levels of pro-(*IL-6*) and anti-inflammatory (*IL-10*) cytokine genes were analyzed in both cA-MSCs and PBMCs (**Fig. 4D-G**). In cA-MSCs, *IL-6* expression was significantly lower in the groups co-cultured with PBMCs than in those that were not. In PBMCs, *IL-6* levels were significantly ($p < 0.05$) higher in allogeneic PBMCs than in autologous PBMCs, regardless of PHA treatment. In cA-MSCs, *IL-10* expression was significantly ($p < 0.05$) lower in the groups co-cultured with autologous PBMCs compared to levels in those that were not (**Fig. 4E**). In PBMCs, *IL-10* expression did not significantly ($p < 0.05$) differ between the allogeneic and autologous PBMC groups (**Fig. 4G**).

Thus, the expression of immunosuppressive (**Fig. 4H-J**) and apoptosis-related genes (**Fig. 4K-N**) were compared at various time points among groups (control [cA-MSCs alone], group 1 [cA-MSCs with allogeneic PBMCs], and group 2 [cA-MSCs with autologous PBMCs]). In all cases, PBMCs were activated with PHA. *IDO*, *PTGS2*, and prostaglandin E synthase (*PTGES*) expression was significantly ($p < 0.05$ and $p < 0.01$) higher in group 1 compared to control from days 1–3, especially on day 1. *PTGES* expression continuously increased in group 1 compared with that of the control group until day 3. However, group 2 exhibited a slight increase in *IDO* and *PTGS2* expression compared to control group levels on day 1.

The expression of caspase-8 (*CASP8*), an initiator of apoptosis, was significantly ($p < 0.05$) higher in group 1 (1.7-fold) than in the other groups on day one and gradually decreased until day 3 (**Fig. 4K**). However, *CASP8* expression in group 2 did not significantly differ from that of the control group ($p > 0.05$) until day 2, although it was significantly ($p < 0.05$) lower on day 3.
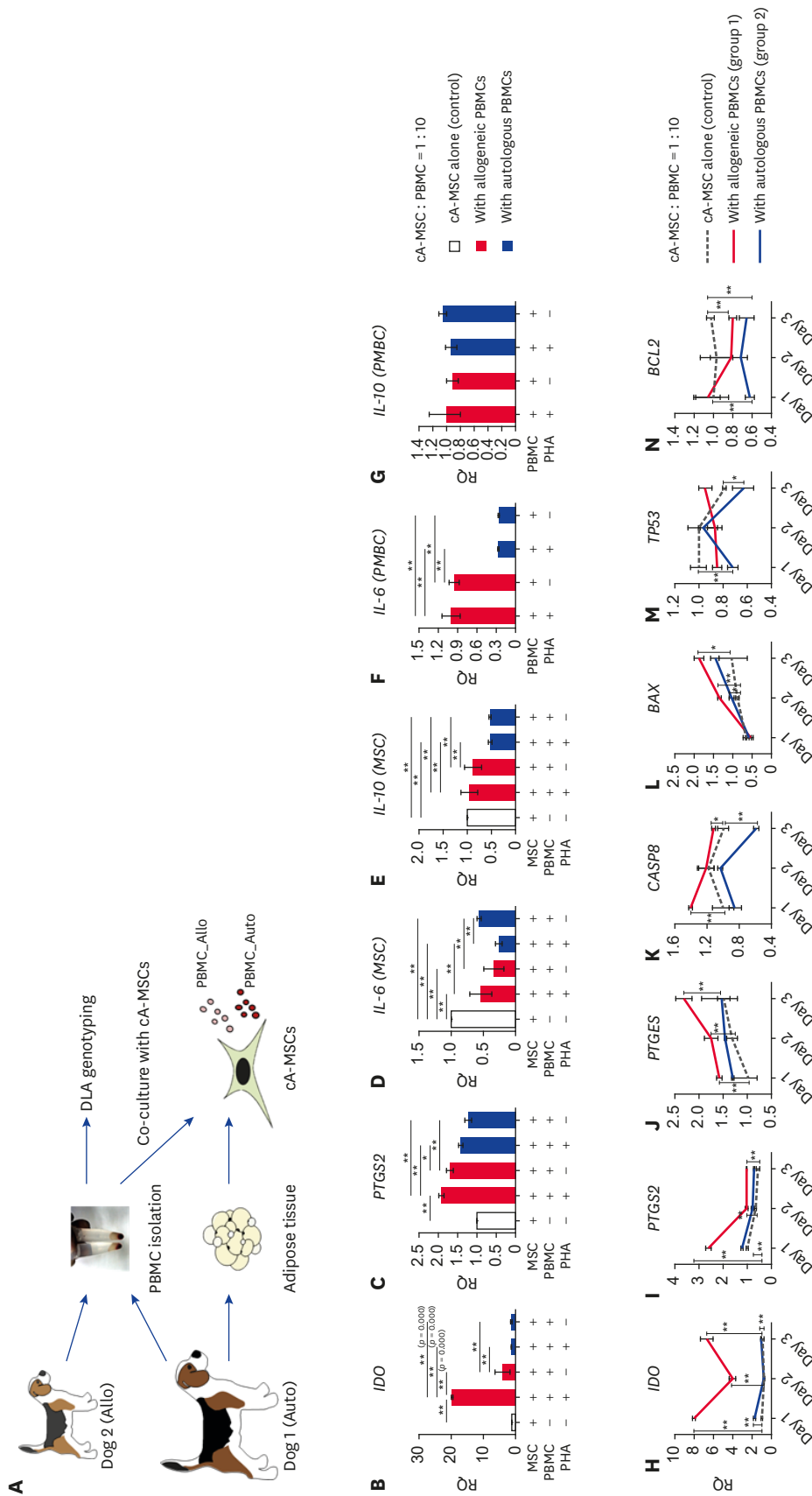
**Fig. 4.** Expression of immunosuppressive, inflammatory, and apoptosis-related genes based on MLR tests between cA-MSCs and PBMCs.
(A) Schematic diagram of the tissue collection and isolation of cells for the MLR testing. The dilution ratio of PBMCs ($0.2 \times 10^6$ cells) and cA-MSCs ($0.2 \times 10^5$ cells) was 10:1. The 2 cell types were co-cultured for 3 days, then each cell type was isolated for specific gene expression analyses. The expression levels of immunosuppressive (B, IDO; C, PTGS2), pro-inflammatory (D and F, IL-6) and anti-inflammatory (E and G, IL-10) genes analyzed on day three via the MLR test. PBMCs were treated with or without PHA (5 μg/mL) to induce their activation. The groups compared consist of cA-MSCs alone (open bars), cA-MSCs treated with allogeneic PBMCs (red bars), and cA-MSCs treated with autologous PBMCs (blue bars). Specific mRNA analysis in cA-MSCs treated with activated PBMCs at 24 h intervals for 3 days. Quantification of immunosuppressive genes (H, IDO; I, PTGS2 and J, PTGES), which are involved in the synthesis of PGE2 and apoptosis-related genes (K, CASP8; L, BAX; M, TP53; N, BCL2) at each time point. The groups compared consist of cA-MSCs alone (black dotted line, control), cA-MSCs treated with allogeneic PBMCs (solid red line, group 1), and autologous PBMCs (solid blue line, group 2).
All experiments were performed in triplicates. Error bars display the minimum and maximum values of RQ.
MLR, mixed lymphocyte reaction; cA-MSCs, canine adipose-derived mesenchymal stem cells; PBMCs, peripheral blood mononuclear cells; IDO, indoleamine 2,3-dioxygenase; PTGS2, prostaglandin-endoperoxide synthase 2; IL, interleukin; PTGES, prostaglandin E synthase; PGE2, prostaglandin E2; CASP8, caspase-8; BAX, Bcl-associated X protein; TP53, tumor protein 53; BCL2, B-cell lymphoma 2; RQ, relative quantification of mRNA.
*$p < 0.05$ and **$p < 0.01$ indicate significant differences among groups at the same time point.

On day 3, the expression of another apoptosis initiator, tumor protein 53 (*TP53*), was slightly upregulated in group 1 compared with that in the control and was slightly downregulated in group 2 compared with levels in the control group (**Fig. 4M**). The TP53 mediator and apoptotic activator Bcl-associated X protein (*BAX*) expression levels were significantly higher in group 1 than in the control group from days 2–3. However, they were slightly increased in group 2 compared with levels in the control group on day 2 (**Fig. 4L**). The expression of inhibitors of *BAX*, *BCL2* was significantly ($p < 0.05$) lower in group 1 than control on day 3, Whereas *BCL2* expression in group 2 was significantly ($p < 0.05$) lower than that in the control group on days 1 and 3.

## DISCUSSION

This study's ultimate goal was to develop a safe, effective, and sustainable method of canine MSC administration, with a lower risk of immune rejection, for use in animal hospitals. Although this study did not investigate cA-MSC transfusions based on DLA type matching *in vivo*, the methodology was indirectly tested under similar environmental conditions *in vitro*. The degree of immune response depends on the source from which MSCs are derived, such as adipose tissue, bone marrow, umbilical cord blood or tissue, or dental pulp stem cells. When recipients repeatedly receive allogeneic bone marrow-derived MSCs transfusions, an increase in cytotoxic (CD8+T cell) and regulatory T cells is induced, which does not occur with allogeneic A-MSCs [14,21]. Therefore, this study used adipose tissue as the MSC source.

Small adipose tissues were isolated and cultured until passage 5 *in vitro*. Characterization revealed the following properties: weak expression of pluripotent stem cells (OCT4, SOX2, and NANOG) and 87% or a higher expression of specific MSC CD markers (CD45⁻, CD44⁺, CD90⁺, and CD29⁺), and the differentiation of three mesodermal origin cell types, including adipocytes, osteocytes, and chondrocytes. However, some tissue-specific genes, including *PPARγ*, *ALP*, and *LPL* exhibited low expression, contrary to expectations. Different induction times for differentiation, individual variabilities, and different reference points could explain these outcomes [22,23]. This study analyzed the cells after 4 weeks of differentiation, whereas some assessed earlier time points [22,24]. Based on these findings, these cells were determined to be cA-MSCs and were used for further studies.

The high number of canine breeds results in greater variability than in humans. DLA types have only been evaluated in some varieties, even though administrated DLA antigens could result in immunogenicity in recipients [25,26]. Based on previous studies, the DLA type, which is the criterion for a successful allograft, was selected; some examples include DLA-88 of DLA class I, and DQA1, DQB1, and DRB1 of DLA class II, all of which exhibit a high degree of polymorphism [3,27,28]. Our results were consistent with previous findings, confirming the two dogs were not siblings based on both the mismatching of analyzed DLA class II types and their family tree; however, despite being based on known literature, the DLA class I genotyping of DLA 88 failed, possibly due to the high degree of genetic polymorphisms and the GC richness in of DLA 88, and differences in the analytical methods [27,28]. Further studies are needed to develop an easy and convenient analytical technique for DLA 88 genotyping.

The immune tolerance of MSCs plays a major functional role in tissue regeneration, as MSCs secrete a variety of soluble paracrine factors, including tumor growth factor beta 1, prostaglandin E2 (PGE2), hepatocyte growth factor (HGF), IDO, nitric oxide (NO), and

IL-10, which alleviate inflammatory responses attributed to innate immune cells [1,29-31] and improve the regenerative capacity of damaged tissue via cell-to-cell communication at gap junctions [4,32]. Furthermore, they alleviate T cell-related innate and adaptive immune activation by inhibiting extrinsic cell death signaling through the binding of the cytotoxic T lymphocyte-expressed Fas ligand (FasL) and its receptor (FasR) [33,34]. This study demonstrated that treating cA-MSCs with allogeneic PBMCs induced an increase in immunosuppressive gene expression, including *PTGS2* (COX2) and *PTGES*, which are involved in *PGE2* synthesis, and *IDO* (8–20-fold increase) compared to changes induced by autologous PBMC treatment. Therefore, allogeneic cA-MSCs exhibited immune tolerance, although this could also potentially weaken the ability to suppress cancer development [35].

cA-MSCs were assumed to inhibit the inflammatory response by decreasing the expression of the pro-inflammatory gene *IL-6* when cA-MSCs were co-cultured with PBMCs. This effect was greater in cell types with matching DLA, and the decreased expression of the anti-inflammatory gene *IL-10* enhanced this response in cA-MSCs treated with autologous PBMCs.

An increase in *CASP8* expression in cA-MSCs treated with allogeneic PBMCs indicated that the extrinsic apoptosis pathway was reinforced by the binding of FasL/FasR in the intrinsic apoptosis pathway. This increased apoptotic signaling occurred downstream of *CASP8*, involving the activation of the pro-apoptotic factor *BAX* and the downregulation of anti-apoptotic *BCL2*. TP53 another apoptotic gene has a low expression level in cA-MSCs treated with PBMCs, especially autologous PBMCs. Therefore, allogeneic cA-MSCs are assumed to have affected cell death by altering *CASP8* rather than *TP53* signaling.

This study revealed that allogeneic cA-MSCs exerted a greater immunosuppressive effect than autologous cA-MSCs through the upregulation of *IDO* and *PTGS2/PTGES* involved in synthesis of PGE2, and the reduction in the pro-inflammatory response via the inhibition of *IL-6*. However, the rapid increase in IDO expression could be a risk factor, as it creates a favorable environment for cancer cell growth. Autologous cA-MSCs exhibited a slight increase in expression of both IDO and the synthesis genes of PGE2 and a lower expression of inflammatory genes than levels in the allogeneic cA-MSCs. Therefore, for safe, efficient, and consistent cA-MSC treatment in animal hospitals, it is necessary banking and database construction of cA-MSCs with variety of DLA types. This study was limited by the small sample size, and further studies are needed with larger populations.

## REFERENCES

1. Dias IE, Pinto PO, Barros LC, Viegas CA, Dias IR, Carvalho PP. Mesenchymal stem cells therapy in companion animals: useful for immune-mediated diseases? BMC Vet Res. 2019;15(1):358.
   **PUBMED** | **CROSSREF**

2. Ogliari KS, Marinowic D, Brum DE, Loth F. Stem cells in dermatology. An Bras Dermatol. 2014;89(2):286-291.
   **PUBMED** | **CROSSREF**

3. Iohara K, Utsunomiya S, Kohara S, Nakashima M. Allogeneic transplantation of mobilized dental pulp stem cells with the mismatched dog leukocyte antigen type is safe and efficacious for total pulp regeneration. Stem Cell Res Ther. 2018;9(1):116.
   **PUBMED** | **CROSSREF**

4. Kot M, Baj-Krzyworzeka M, Szatanek R, Musiał-Wysocka A, Suda-Szczurek M, Majka M. The importance of HLA assessment in "off-the-shelf" allogeneic mesenchymal stem cells based-therapies. Int J Mol Sci. 2019;20(22):5680.
   **PUBMED** | **CROSSREF**

5. Pittenger MF, Mackay AM, Beck SC, Jaiswal RK, Douglas R, Mosca JD, et al. Multilineage potential of adult human mesenchymal stem cells. Science. 1999;284(5411):143-147.
   **PUBMED | CROSSREF**

6. Di Nicola M, Carlo-Stella C, Magni M, Milanesi M, Longoni PD, Matteucci P, et al. Human bone marrow stromal cells suppress T-lymphocyte proliferation induced by cellular or nonspecific mitogenic stimuli. Blood. 2002;99(10):3838-3843.
   **PUBMED | CROSSREF**

7. Drukker M, Katz G, Urbach A, Schuldiner M, Markel G, Itskovitz-Eldor J, et al. Characterization of the expression of MHC proteins in human embryonic stem cells. Proc Natl Acad Sci U S A. 2002;99(15):9864-9869.
   **PUBMED | CROSSREF**

8. Bocelli-Tyndall C, Zajac P, Di Maggio N, Trella E, Benvenuto F, Iezzi G, et al. Fibroblast growth factor 2 and platelet-derived growth factor, but not platelet lysate, induce proliferation-dependent, functional class II major histocompatibility complex antigen in human mesenchymal stem cells. Arthritis Rheum. 2010;62(12):3815-3825.
   **PUBMED | CROSSREF**

9. Wang RF. The role of MHC class II-restricted tumor antigens and CD4^{+} T cells in antitumor immunity. Trends Immunol. 2001;22(5):269-276.
   **PUBMED | CROSSREF**

10. Wilbe M, Jokinen P, Hermanrud C, Kennedy LJ, Strandberg E, Hansson-Hamlin H, et al. MHC class II polymorphism is associated with a canine SLE-related disease complex. Immunogenetics. 2009;61(8):557-564.
    **PUBMED | CROSSREF**

11. Poncelet AJ, Vercruysse J, Saliez A, Gianello P. Although pig allogeneic mesenchymal stem cells are not immunogenic *in vitro*, intracardiac injection elicits an immune response *in vivo*. Transplantation. 2007;83(6):783-790.
    **PUBMED | CROSSREF**

12. Cuervo B, Rubio M, Sopena J, Dominguez JM, Vilar J, Morales M, et al. Hip osteoarthritis in dogs: a randomized study using mesenchymal stem cells from adipose tissue and plasma rich in growth factors. Int J Mol Sci. 2014;15(8):13437-13460.
    **PUBMED | CROSSREF**

13. Harman R, Carlson K, Gaynor J, Gustafson S, Dhupa S, Clement K, et al. A prospective, randomized, masked, and placebo-controlled efficacy study of intraarticular allogeneic adipose stem cells for the treatment of osteoarthritis in dogs. Front Vet Sci. 2016;3:81.
    **PUBMED | CROSSREF**

14. Kol A, Wood JA, Carrade Holt DD, Gillette JA, Bohannon-Worsley LK, Puchalski SM, et al. Multiple intravenous injections of allogeneic equine mesenchymal stem cells do not induce a systemic inflammatory response but do alter lymphocyte subsets in healthy horses. Stem Cell Res Ther. 2015;6(1):73.
    **PUBMED | CROSSREF**

15. Bunnell BA, Flaat M, Gagliardi C, Patel B, Ripoll C. Adipose-derived stem cells: isolation, expansion and differentiation. Methods. 2008;45(2):115-120.
    **PUBMED | CROSSREF**

16. Marędziak M, Śmieszek A, Chrząstek K, Basinska K, Marycz K. Physical activity increases the total number of bone-marrow-derived mesenchymal stem cells, enhances their osteogenic potential, and inhibits their adipogenic properties. Stem Cells Int. 2015;2015:379093.
    **PUBMED | CROSSREF**

17. Barry F, Boynton RE, Liu B, Murphy JM. Chondrogenic differentiation of mesenchymal stem cells from bone marrow: differentiation-dependent gene expression of matrix components. Exp Cell Res. 2001;268(2):189-200.
    **PUBMED | CROSSREF**

18. Murgia C, Pritchard JK, Kim SY, Fassati A, Weiss RA. Clonal origin and evolution of a transmissible cancer. Cell. 2006;126(3):477-487.
    **PUBMED | CROSSREF**

19. Kennedy LJ, Barnes A, Short A, Brown JJ, Lester S, Seddon J, et al. Canine DLA diversity: 1. New alleles and haplotypes. Tissue Antigens. 2007;69 Suppl 1:272-288.
    **PUBMED | CROSSREF**

20. Livak KJ, Schmittgen TD. Analysis of relative gene expression data using real-time quantitative PCR and the $2^{-\Delta\Delta Ct}$ Method. Methods. 2001;25(4):402-408.
    **PUBMED | CROSSREF**

21. Lee M, Jeong SY, Ha J, Kim M, Jin HJ, Kwon SJ, et al. Low immunogenicity of allogeneic human umbilical cord blood-derived mesenchymal stem cells *in vitro* and *in vivo*. Biochem Biophys Res Commun. 2014;446(4):983-989.
   **PUBMED | CROSSREF**

22. Ock SA, Maeng GH, Lee YM, Kim TH, Kumar BM, Lee SL, et al. Donor-matched functional and molecular characterization of canine mesenchymal stem cells derived from different origins. Cell Transplant. 2013;22(12):2311-2321.
   **PUBMED | CROSSREF**

23. Bertolo A, Steffen F, Malonzo-Marty C, Stoyanov J. Canine mesenchymal stem cell potential and the importance of dog breed: implication for cell-based therapies. Cell Transplant. 2015;24(10):1969-1980.
   **PUBMED | CROSSREF**

24. Russell KA, Chow NH, Dukoff D, Gibson TW, LaMarre J, Betts DH, et al. Characterization and immunomodulatory effects of canine adipose tissue- and bone marrow-derived mesenchymal stromal cells. PLoS One. 2016;11(12):e0167442.
   **PUBMED | CROSSREF**

25. Hardt C, Ferencik S, Tak R, Hoogerbrugge PM, Wagner V, Grosse-Wilde H. Sequence-based typing reveals a novel DLA-88 allele, DLA-88*04501, in a beagle family. Tissue Antigens. 2006;67(2):163-165.
   **PUBMED | CROSSREF**

26. Tsai KL, Starr-Moss AN, Venkataraman GM, Robinson C, Kennedy LJ, Steiner JM, et al. Alleles of the major histocompatibility complex play a role in the pathogenesis of pancreatic acinar atrophy in dogs. Immunogenetics. 2013;65(7):501-509.
   **PUBMED | CROSSREF**

27. Venkataraman GM, Kennedy LJ, Little ME, Graves SS, Harkey MA, Torok-Storb BJ, et al. Thirteen novel canine dog leukocyte antigen-88 alleles identified by sequence-based typing. HLA. 2017;90(3):165-170.
   **PUBMED | CROSSREF**

28. Miyamae J, Suzuki S, Katakura F, Uno S, Tanaka M, Okano M, et al. Identification of novel polymorphisms and two distinct haplotype structures in dog leukocyte antigen class I genes: *DLA-88*, *DLA-12* and *DLA-64*. Immunogenetics. 2018;70(4):237-255.
   **PUBMED | CROSSREF**

29. Chabannes D, Hill M, Merieau E, Rossignol J, Brion R, Soulillou JP, et al. A role for heme oxygenase-1 in the immunosuppressive effect of adult rat and human mesenchymal stem cells. Blood. 2007;110(10):3691-3694.
   **PUBMED | CROSSREF**

30. Yagi H, Soto-Gutierrez A, Parekkadan B, Kitagawa Y, Tompkins RG, Kobayashi N, et al. Mesenchymal stem cells: mechanisms of immunomodulation and homing. Cell Transplant. 2010;19(6):667-679.
   **PUBMED | CROSSREF**

31. Gao F, Chiu SM, Motan DA, Zhang Z, Chen L, Ji HL, et al. Mesenchymal stem cells and immunomodulation: current status and future prospects. Cell Death Dis. 2016;7(1):e2062.
   **PUBMED | CROSSREF**

32. de Windt TS, Saris DB, Slaper-Cortenbach IC, van Rijen MH, Gawlitta D, Creemers LB, et al. Direct cell-cell contact with chondrocytes is a key mechanism in multipotent mesenchymal stromal cell-mediated chondrogenesis. Tissue Eng Part A. 2015;21(19-20):2536-2547.
   **PUBMED | CROSSREF**

33. Atsuta I, Liu S, Miura Y, Akiyama K, Chen C, An Y, et al. Mesenchymal stem cells inhibit multiple myeloma cells via the Fas/Fas ligand pathway. Stem Cell Res Ther. 2013;4(5):111.
   **PUBMED | CROSSREF**

34. Kim JH, Lee YT, Hong JM, Hwang YI. Suppression of *in vitro* murine T cell proliferation by human adipose tissue-derived mesenchymal stem cells is dependent mainly on cyclooxygenase-2 expression. Anat Cell Biol. 2013;46(4):262-271.
   **PUBMED | CROSSREF**

35. Liu H, Shen Z, Wang Z, Wang X, Zhang H, Qin J, et al. Increased expression of IDO associates with poor postoperative clinical outcome of patients with gastric adenocarcinoma. Sci Rep. 2016;6(1):21319.
   **PUBMED | CROSSREF**